Desalination 438 (2018) 24–36

Contents lists available at ScienceDirect

Desalination

journal homepage: www.elsevier.com/locate/desal

A parametric study of multiscale transport phenomena and performance characteristics of capacitive deionization systems☆

Yasamin Salamat, Carlos H. Hidrovo*

Mechanical and Industrial Engineering Department, Northeastern University, 334 Snell Engineering Center, 360 Huntington Ave, Boston, MA 02115, USA

GRAPHICAL ABSTRACT

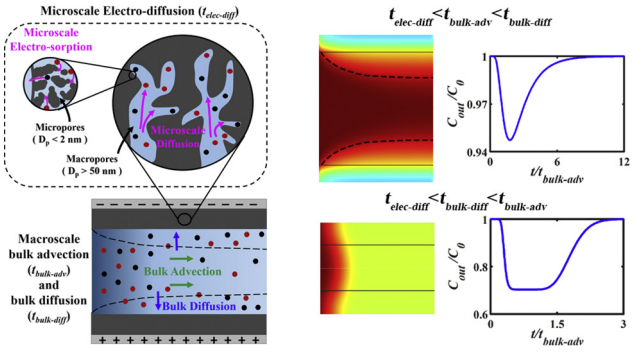

ARTICLE INFO

Keywords:
Capacitive deionization
Desalination performance
Porous-electrode regeneration
Energy efficiency

ABSTRACT

Capacitive deionization (CDI) is a relatively novel desalination technology which uses electrically charged porous electrodes to remove ions from low salinity water streams. The interplay between the micro- and macroscale transport mechanisms in the porous electrodes and bulk flow of the CDI unit dictates the concentration profile at the exit. A thorough understanding of these interactions is important towards achieving high-efficiency systems. Through permutation of the associated transport time constants, we conduct a parametric study to investigate the coupling of multiscale phenomena in CDI. Moreover, we propose a new multi-cycle arrangement to further improve the desalination performance of a given saline solution. In these systems, the regeneration feed stream used for each cycle highly affects the efficiency of the whole system, as it directly affects the water recovery ratio, the total duration of the process, and the desalination performance of the next cycle. We propose three regeneration schemes, with different regeneration feed streams to enhance the desalination/regeneration performance of the multi-cycle arrangements. To obtain comprehensive characterization of desalination and regeneration performances of different units, we introduce new inclusive metrics that encompass different aspects of the system. The results indicate trade-offs between desalination performance and energy efficiency of the proposed arrangements.

1. Introduction

Meeting the ever-growing water demands of the planet population with the limited available resources is one of the major crisis worldwide. In addition to significant rise in the amount of water required by the agriculture sector, which consumes near 70% of the total fresh

☆ Supplementary information available: Figure of outlet concentration profile in cases with two or three time constants at the same order of magnitude.

* Corresponding author.
E-mail address: hidrovo@neu.edu (C.H. Hidrovo).

https://doi.org/10.1016/j.desal.2018.03.022
Received 12 November 2017; Received in revised form 1 March 2018; Accepted 21 March 2018

water withdrawn globally, unprecedented water demands specifically in industry and energy management are anticipated in the near future [1,2]. On average over 80% of the total municipal and industrial wastewater around the world is discarded into the environment without sufficient post-treatment. The situation is more severe in low-income countries where low-cost water treatment techniques are of great importance [2]. This along with the fact that around 97.5% of the total water on Earth is either brackish or sea water [3] have attracted considerable attention towards water desalination to increase both quantity and quality of the water required in many applications [2,4–7]. Electro-sorption techniques, such as Capacitive Deionization (CDI) represent highly efficient and low-cost alternatives to common desalination methods, namely Reverse Osmosis (RO), Multi-Effect Distillation (MED), and Multi-Stage Flash Distillation (MSF) for desalinating low salinity brackish water, defined as a water with total salt concentration of 0.5–35 mg/ml [5,8–10].

CDI is a novel desalination technique in which an electrical field is employed to separate ions from stream of an ionic solution by adsorbing them into porous media [5,11–17]. As water is pumped through a CDI unit, a relatively low DC voltage (1–1.2 V, below the electrolysis voltage of the water molecules) is used to apply an electrical field. Ionic species are consequently attracted to the charged, highly-porous electrodes. Thus, the concentration of the output solution decreases until the electrodes are saturated with the ionic species. During the electro-sorption of counterions, electric energy is stored in the porous media that can partly be recovered during a regeneration step. The electrodes can be regenerated by electrically discharging to an electrical load or storage element (i.e., a capacitor). Regeneration of the electrodes can also be done by reducing the applied voltage or even applying a reverse voltage [13,18–22]. Previously, it was argued that using the latter discharging (regeneration) approach is not feasible in CDI as the ions released from one electrode can get quickly re-adsorbed into the opposite electrode before they exit the unit [23,24]. However, later studies proved the efficacy of this regeneration method for discharging the CDI cells [13,18–20]. Although this approach improves the charge efficiency of the system, it reduces the adsorption rate during desalination [13,20]. Moreover, Kim et al. showed that regenerating the electrodes by applying a voltage lower than the desalination voltage (but with the same polarity) also enhances the charge efficiency [25]. Along with its ability to retrieve part of the consumed energy, CDI has some distinct features as compared to conventional desalination methods, such as RO and MSF. Due to the small working voltage window, CDI units require lower energy input and capital costs for treating brackish water [5,11,12,26–28]. Furthermore, as there is no membrane or delicate and complex features involved in the process, it demands less maintenance.

Electro-sorption and diffusion of ionic species in the porous electrodes set the concentration and electric potential boundary conditions at the interface of the electrodes and the main bulk solution, and therefore, highly affect the advection and transverse diffusion of ions in the bulk flow. In other words, interplay of various transport mechanisms in CDI dictate the performance of the system under different conditions. Hence, deep understanding of desalination regimes is highly crucial to obtain the most efficient CDI system for different applications. So far, comprehensive studies have been conducted to understand the physics underlying the electro-sorption process in the Electrical Double Layers (EDLs) of the microporous electrodes. Nernst-Planck (NP) equations and time-dependent Gouy-Chapman-Stern (GCS) models have been employed to describe the electro-sorption of charged species in a CDI unit [13,29–36]. Biesheuvel et al. asserted that while ion transport can be modeled by Nernst-Planck theory and electroneutrality assumption within the electrode's macropores, in the micropores with highly overlapped EDLs the adsorption process can be explained by the modified Donnan (mD) model [37]. Similar to the classical Donnan model, the mD model considers a potential drop between the inside and outside of the micropores and assumes uniform potential and concentration profile within the micropores. Nevertheless, the mD model deviates from the classical Donnan approach in two ways. First by including a Stern layer between the electronic charge at the surface of the electrode and the ionic charge in the micropores, and secondly by considering a non-electrostatic attraction term to better fit the experimental data to the model [13,17,38,39].

Guyes et al. introduced an 1D improved Donnan (i-mD) model in which they simplified the boundary conditions by scaling arguments and argued that including the electrolyte volume and diffusion dynamics downstream of such cells is necessary to better describe the experimental data [40]. Rios Perez et al., on the other hand, developed a one-dimensional macroscale model based on the Nernst-Planck equation and mass conservation analysis describing the mass transfer within the bulk solution during a desalination cycle in CDI [41]. Nevertheless, this model does not take into account the transport of the ions within the porous electrodes.

Biesheuvel et al. further extended the mD model and developed an amphoteric Donnan model which includes immobile chemical charges with different signs at the surface of the electrodes' matrix in the micropores [42,43]. Based on the amphoteric Donnan model and using an euler backward approach, Dysktra et al. developed a 2D model which considers only advection of the species in the direction of the flow in the main channel and fully solves the Nernst-Planck equation in the direction perpendicular to the flow [44]. Their model fits well to the experimental data and they used it to calculate the ionic resistances in the system. Later, they improved the model by exploiting acid-base equilibrium reactions to describe pH changes during water desalination process [45]. Based on the mD approach, Hemmatifar et al. proposed a two-dimensional model which couples mass, ionic and electronic charge transport describing the adsorption and desorption of charged species in CDI [46]. They presented numerical estimation of the adsorption/desorption dynamics in the micro- and macropores for both high and low inlet salt concentrations. However, they did not discuss the effects of transport mechanisms in porous media on the bulk solution, away from the electrodes' surface and on the outlet stream of the CDI unit.

Despite the critical insight provided by the existing models in the literature, there is no comprehensive analysis on the interplay between microscale and macroscale transport phenomena in different desalination regimes. In this paper, by permutation of the transport time constants and implementing the two-dimensional porous electrode model developed by Hemmatifar et al. [46], we conduct a parametric study to investigate the interactions between microscale and macroscale motions of ionic species in flow-by CDI systems with various configurations. To focus on how rates of the main transport mechanisms in CDI cells affect concentration of the effluent, we investigate 13 desalination cases with different characteristic timescales.

Thus far, different metrics have been proposed by both theoretical and experimental researches to evaluate the performance of CDI-based water desalination systems [17,47–49]. Initial studies on CDI have mainly focused on the amount of salinity reduction [50,51]. While this metric is directly associated with the ability of a system to reduce the concentration of the inlet stream, it does not provide sufficient data about other desalination and regeneration characteristics of the CDI system such as rate of desalination or amount of treated water. To make a more inclusive analysis of CDI systems, further studies proposed additional metrics such as maximum salt adsorption capacity (*mSAC*) [48,52], charge capacity [53–55], average salt adsorption rate (*ASAR*) [15,56,57], and charge and current efficiency [16,31,49,58,59]. Although the amount of the salt adsorbed and the rate of adsorption appear to be the intuitive means of comparison among desalination systems, by considering them independently no conclusion can be made regarding the overall performance of different systems. In this work, we propose new metrics that incorporate desalination percentage, volume of treated water, ion removal rate, water recovery ratio, and the total duration of the process into a unified metric. Using these metrics, we

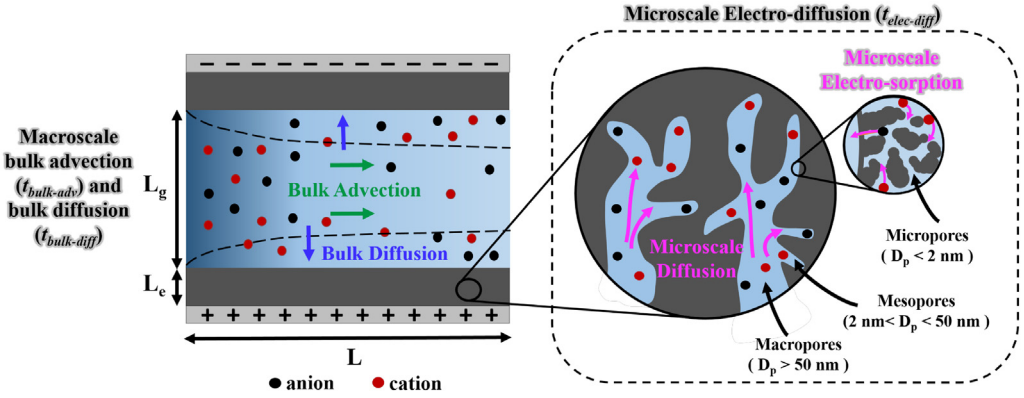

Fig. 1. Schematic representation of macroscale and microscale transport phenomena in the main bulk flow channel and the microporous electrodes of a CDI cell. Associated with the transport mechanisms, three distinct timescales are considered in this study. The bulk advection timescale ($t_{bulk-adv}$), defined as L/U, considers motion of the salt species through the cell due to the bulk flow. The bulk diffusion timescale ($t_{bulk-diff}$), defined as $(L_g/2)^2/D_{bulk}$, accounts for the diffusion of the species from the main channel towards the electrodes. Lastly, the electro-diffusion timescale ($t_{elec-diff}$) correlates with diffusion and electro-sorption of the ions within the porous electrode and is defined using Eq. (2).

perform a comprehensive comparison on the desalination and regeneration performance of different CDI systems.

CDI experiments usually adopt either a batch-mode (BM) or a single-pass (SP) approach to desalinate water. In BM, the effluent of the CDI unit is returned to the feeding reservoir, where the conductivity is measured [13,17,60,61]. Volume of the recycling reservoir for this method, whose initial salinity is usually low (< 5 mM), must be small enough so the change in the conductivity is distinguishable. The measured conductivity constantly decreases in this technique until it reaches a low, steady value which indicates saturation of the electrodes. In contrast, in the SP approach the conductivity of the treated water is measured directly at the exit of the CDI unit and the effluent of the system is either discarded or returned to the feeding reservoir which is sufficiently big so that adding the outlet solution does not change its salinity substantially [13,17,33]. In this approach, each desalination stage can be conducted before or until full saturation of the porous electrodes is achieved [13,20,25,55]. Different studies have incorporated the SP method with multiple repeated full desalination and regeneration cycles [13,15,25,58,62]. Most of these cyclic CDI systems solely served to obtain a better understanding of CDI performance and energy consumption under dynamic equilibrium (a state at which the amount of salt adsorbed during desalination is equal to the amount of salt desorbed during the regeneration process) [13,25,58,62], or to investigate reduction in adsorption capacity of porous electrodes after multiple repeated full cycles [15]. Recently, some attempts have been made to use sequential CDI cycles to decrease the concentration of the main reservoir more than what is achieved through one desalination cycle. Lado et al. explored a multi-cycle method of operation in which the first cycle is carried out until the minimum concentration is reached [21]. After the following regeneration step, the subsequent desalination cycles were operated for a shorter time. Although they achieved lower salinity comparing to a single-step system, they provided no systematic approach that can be applied to other multi-cycle arrangements for determining the termination point of the desalination processes after the first cycle.

Moreover, a number of studies have focused on the regeneration stage in cyclic arrangements. Desalination performance of CDI systems using the reversed-voltage method for discharging the electrodes was measured against the zero-voltage approach in terms of energy consumption, charge efficiency and desalination percentage [13,20]. In another work, Demirer et al. investigated effects of varying regeneration starting time on the performance of a cyclic CDI system, in terms of ions adsorbed per energy per volume, energy recovery, and thermodynamic efficiency [4]. Recently, a few studies have focused on the effects of the regeneration inlet stream on the energetic performance of the system showing that increasing the concentration of the regeneration feed stream benefits the system in terms of energy consumption [63,64]. However, they mainly focused on how the regeneration feed solution affects the energy recovery of one CDI cycle and did not evaluate its impact on the desalination performance of the next cycle and the overall efficacy of the process in a multi-cycle arrangement.

In this work, to improve the desalination percentage of a given solution using CDI we propose a cyclic system in which the concentration of the influent at each desalination stage is set as the minimum average concentration obtained in the previous cycle. Moreover, to further enhance the overall performance and efficiency of these multi-cycle arrangements, three different regeneration scenarios are introduced. Each of these regeneration schemes differs from the others in terms of the feed stream used for regenerating the CDI cell. We use the proposed metrics to compare the efficacy of these regeneration schemes in various CDI systems.

2. Theory

In this section, we outline the underlying physics of multiscale transport phenomena in a CDI cell, and define the relevant time constants associated with each transport mechanism. Afterwards, the new metrics proposed to evaluate and compare performance of CDI units for different applications are introduced. Lastly, we describe the proposed multi-cycle CDI system and the three regeneration scenarios.

2.1. Transport phenomena and the associated timescales in CDI

The current understanding of transport and adsorption of salt and ionic species in CDI is based on a two-tier pore size model that combines electro-sorption and basic mass diffusion [42,44,46,52]. Fig. 1 shows schematics of the microstructure networks in a porous electrode and the transport mechanisms of ionic species in a sample CDI unit. Following IUPAC terminology, three sets of pore sizes are defined in porous media: macropores, mesopores, and micropores, whose dimensions are > 50 nm, between 2 and 50 nm, and < 2 nm, respectively. The model implemented in this work is developed based on a form of the mD theory which can be applied for bimodal porous structures consisting of micro- and macropores only. The primary difference between the two stems from the physical extent of the EDL (1–10 nm) in relationship to the pore size. In the macropores, the EDL thickness is negligible compared to the pore size while the EDLs highly overlap each other in the micropores. Therefore, contrary to the condition in the micropores, charge neutrality can be assumed in the macropores.

Initially, before applying the electrical field in the system the macro- and micropores are filled with the ionic solution. Upon applying the voltage, owing to the extremely overlapped EDLs in the micropores, counter-ions are adsorbed to the surface of the electrode while co-ions with the same electric charge as the adjacent electrode are repelled from it. Due to the concurrent attraction of counter-ions and repulsion of co-ions in the micropores, regions with depleted salt concentration form in the macropores. This concentration depletion leads to a diffusion-based movement of species within the thickness of the electrode

which subsequently gives rise to the diffusion of salt species in the main channel towards the interface of the electrode and the bulk flow. In addition to these transport mechanisms in the porous electrodes, advection of the ionic species takes place in a flow-by system due to the flow in the main channel. Desorption of the species during the regeneration stage occurs in a relatively similar but reverse manner. Upon short circuiting the electrodes, which is the regeneration method adopted in this work, previously-adsorbed counter-ions in the micropores are quickly discharged to compensate the zero voltage at the surface of the electrode. The excess ionic species adsorbed in the desalination phase eventually exit the system by means of diffusion from the electrodes into the main channel and advection within the bulk flow. In this system, the diffusion and electro-sorption of charged species taking place in the macro- and micropores, respectively, are merged into one transport mechanism and referred as the microscale electro-diffusion. Additionally, the macroscale advection and transverse diffusion of the salt species in the main channel are considered as the bulk advection and bulk diffusion, respectively, and are referred as the bulk flow transport mechanisms.

Three time constants can be associated with the motion of species in a CDI unit, correlated with different transport mechanisms. The advection timescale, $t_{bulk\text{-}adv}$, is related to the flow of the bulk solution through the main channel and can be calculated as L/U, where L is the total length of the flow channel and U is the average velocity of the stream. The transverse diffusion timescale, $t_{bulk\text{-}diff}$, is associated with the diffusion of the species in the bulk solution towards the electrodes and is expressed as $(L_g/2)^2/D_{bulk}$, where L_g is the gap distance between the two porous electrodes, and D_{bulk} is the diffusion coefficient of salt species in the bulk solution. The electro-diffusion time constant, $t_{elec\text{-}diff}$, is related to the transport of the species within the electrodes which comprises both the resistance and capacitance associated with the charging process of the electrodes. Despite the existence of a transport resistance from the macropores into the micropores, this resistance is neglected here and in all the previous work, considering only the transport resistance in the macropores. Thus, $t_{elec\text{-}diff}$ takes into account the resistivity and capacity related to the diffusion in the macropores and the electro-sorption in the micropores, respectively.

In the charging process of the porous electrodes in CDI described by the mD model, the diffusion of the species throughout the macropores (neglected EDLs) is coupled to their electro-sorption in the micropores (highly overlapped EDLs) and the relation between micropores and macropores concentrations is governed by a Boltzmann distribution. This is similar to the charging of an EDL, where the attraction of the counter-ions and repulsion of the co-ions are balanced by the diffusion of the ionic species in the electrolyte. Consequently, using this analogy, a characteristic length can be defined for the charging process of the electrodes as:

$$L_D = \sqrt{\frac{\varepsilon RT}{2F^2\, c_{ma}}} \tag{1}$$

where, ε is the permittivity of the medium, R is the universal gas constant, T is the temperature, F is the Faraday constant, and c_{ma} is the concentration in the macropores. The $t_{elec\text{-}diff}$ related to the charging process of the electrodes is defined as ${L_D}^2/D_{elec}$, where D_{elec} is the effective diffusivity of the solution in the porous electrode. The effective diffusion coefficient can be obtained by multiplying D_{bulk} and p_{ma}/τ, where p_{ma} and τ are macropore porosity and tortuosity of the porous electrode, respectively. Assuming τL_e as the effective length of the pores in the electrode, and based on the total capacitance of the electrode obtained as $C_{total} = C(A_e L_e)p_{mi}$ (where C is the capacitance of the electrode per unit volume of the micropores, A_e is the surface area of the electrode, and p_{mi} is the porosity of the micropores), value of the electro-diffusion timescale is calculated as:

$$t_{\mathrm{elec-diff}} = \frac{C\,\tau^2 L_e^2\, V_T}{2F\, D_{\mathrm{bulk}}\, c_{ma,0}} \frac{p_{mi}}{p_{ma}} \tag{2}$$

where V_T is the thermal voltage and is defined as $k_B T/e$, where k_B and e are the Boltzmann constant and the charge of an electron, respectively. The $t_{elec\text{-}diff}$ defined here is analogous to the time constant derived by Suss et al. who accounted for the charging process of the electrodes based on a RC timescale [57]. Moreover, conducting an order of magnitude analysis on the equation corresponding to the conservation of charge in the macropores in the mD model, the same correlation as Eq. (2) can be obtained for the charging process of the electrodes.

The relative magnitude of the abovementioned timescales can be used to characterize the conditions under which the CDI system is performing. Macroscale transport of the salts can be described through macroscale mass Péclet number defined as $Pe_m = t_{bulk\text{-}diff}/t_{bulk\text{-}adv}$. Similarly, the rate of the microscale electro-diffusion of the species in the electrode can be compared to their advection rate in the main channel through the Damköhler number defined as $Da = t_{bulk\text{-}adv}/t_{elec\text{-}diff}$. Lastly, the second Damköhler number, $Da_{II} = t_{bulk\text{-}diff}/t_{elec\text{-}diff}$ can be used to compare microscale electro-diffusion and bulk diffusion rates. In essence, the two latter non-dimensional numbers compare the charging rate of the electrodes to the bulk flow transport rate of the species in the main channel.

The concentration profile in the macro- and micropores during adsorption and desorption cycles have been numerically investigated in the literature. Nevertheless, previous studies have mostly focused on electro-diffusion limited cases and a limited range of CDI configurations have been analyzed. Although Hemmatifar et al. were the first group to develop a general two-dimensional model based on the mD model by solving the Nernst-Planck equations both in the direction of and perpendicular to the flow, they evaluated the coupling of the transport mechanisms only for a fast diffusion and slow advection in the main channel and a relatively slow electro-diffusion in the electrodes. Specifically, in their system, $Pe_m = 0.4$, $Da = 0.3$, and $Da_{II} = 0.1$ ($t_{bulk-diff} < t_{bulk-adv} < t_{elec-diff}$). Furthermore, no inclusive study exists on the effects of the coupling between the bulk flow and porous electrode transport mechanisms on the concentration behavior of the effluent in different CDI configurations. To further investigate the interplay between microscale electro-diffusion and bulk advection and diffusion in CDI we analyze these transport processes for a broader range of Pe_m, Da, and Da_{II}, by implementing the mentioned 2D numerical model.

In a flow-by CDI cell, bulk diffusion of the ions into the porous electrode is in a continuous competition with their bulk advection in the flow direction. The region in which diffusion of the ions towards the porous electrode is more dominant than their advection is called the convective-diffusive layer [41,65]. Like the concept of the hydraulic and thermal boundary layers, a developing and fully developed convective-diffusive layer may be defined in a CDI cell. Fig. 2 depicts concentration profiles of both regimes in a CDI cell. At low flow rates, diffusion of the ions towards the porous electrode is faster than their advection through the cell ($Pe_m < 1$). As such, bulk diffusion is spatially uniform in the transverse direction of the channel, creating a fully developed convective-diffusive layer. However, at high flow rates, the bulk advection transport of the ions along the cell is much faster than their bulk diffusion towards the electrode ($Pe_m > 1$). Therefore, bulk diffusion of ions is primarily confined to the thin developing convective-diffusive layer near the interface of the electrodes and the main stream. In the developing regime, due to high flow rates of the solution stream in the system, advection of the species through the main channel exceeds their diffusion towards the porous media ($t_{bulk-adv} < t_{bulk-diff}$). This results in reaching higher minimum average concentration in a CDI cell with developing convective-diffusive layers compared to the same unit with fully developed regime obtained at lower flow rates [19,41,66].

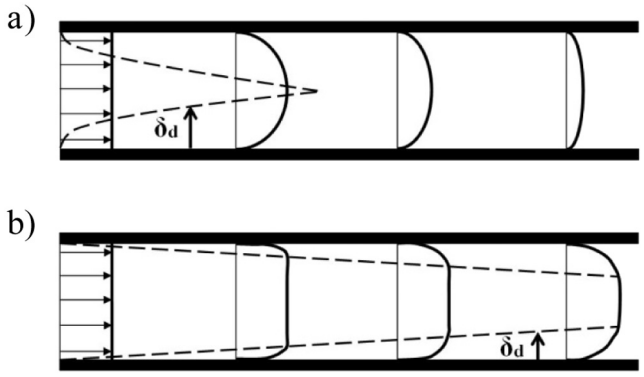

Fig. 2. Concentration profiles in a) fully developed and b) developing convective-diffusive regimes. δ_d represents the thickness of the convective-diffusive layer. At lower Peclet numbers ($Pe_m < 1$), the diffusion of the salt species towards the porous electrode is faster than their advection through the cell, allowing for a fully developed regime where the two convective-diffusive layers merge. In contrast, the developing regime occurs at higher Péclets ($Pe_m > 1$) when the bulk advection of the species along the cell surpasses their bulk diffusion.

2.2. Multi-cycle CDI systems and regeneration schemes

Due to the finite capacitance of the porous electrodes used in CDI, there exists a limit on the total amount of salts that can be removed from a given solution. Because of the space, material, and cost restraints, bigger CDI units having porous electrodes with larger surface area may not be feasible or economical. Consequently, to further decrease the concentration of the feeding solution and benefiting from the ability to regenerate the saturated electrodes, instead of desalinating a specific solution for only 1 cycle, one can run multiple successive full CDI cycles each desalinating the outlet solution of the previous cycle. At each cycle, the desalination purpose can be fulfilled until the average concentration of the total water collected at the outlet of a system is decreasing. At each instant of time, the average concentration of the treated water is calculated as follows:

$$c_{ave} = \frac{1}{t}\int_0^t c(t^*)dt^* \tag{3}$$

where c is the concentration at the exit, and t is the time at which the measurement takes place. Therefore, in this multi-cycle arrangement each desalination step is operated until the minimum average concentration, $c_{ave,min}$, is achieved at the exit of the unit. The electrodes are discharged afterwards, to recover their adsorption capacity. Subsequently, the desalinated solution feeds the next cycle. This procedure can be repeated until the desired concentration is obtained.

Salinity of the regeneration stage plays a significant role in the overall performance of the proposed cyclic CDI systems. Not only the regeneration feed stream affects the discharging time and total amount of consumed water but it also influences desalination performance of the next cycle as it determines the initial conditions at which the adsorption process starts. Other than using the targeted reservoir (whose salinity is intended to decrease) as the regeneration feed stream, one can recover the electrodes employing brine of the regeneration stage in the previous cycle. Using this technique will favor the total volume of water utilized for the process since instead of using the main reservoir for regeneration and discarding the brine at the end of it, it is recycled to be used for the next discharging process. However, a CDI cell with higher salinity solution initially filling the main channel and porous electrodes results in higher average concentration at the exit during the desalination stage. As a result, comparing to a cell with lower salinity initial condition, lower total desalination percentage will be obtained. To increase the overall desalination percentage in the proposed cyclic CDI system one can use the same feeding stream for both desalination and regeneration purposes. Although this will enhance the diffusion of ionic species from the electrodes into the bulk flow during the regeneration process, more water is required to provide sufficient amount for both charging and discharging of the following cycle. Performance of cyclic CDI systems with various operational configurations functioning under the proposed regeneration approaches is investigated here in terms of desalination, water consumption, and duration of the whole process.

The maximum ability of different CDI arrangements in recovering the consumed energy during desalination is evaluated and compared as well. The electrical energy used during desalination stage can be calculated as:

$$E_{\text{used}}(t) = \int_0^t I(t)Vdt \tag{4}$$

where I and V are the electrical current and the applied voltage, respectively. The energy stored during the desalination stage can be calculated using the ionic current and the potential difference between the charged surface of the electrode and the charge-neutral electrolyte in the macropore. In the context of the mD model, this potential difference comprises of the Stern potential and the Donnan potential. The Stern potential $\Delta\varphi_s$ is the potential difference between the surface of the electrode and the micropore and the Donnan potential $\Delta\varphi_D$ is the potential difference between the micro- and macropore. Therefore, the stored energy through the ionic charge can be obtained as:

$$E_{stored,total}(t) = \int_0^t I(\Delta\varphi_s + \Delta\varphi_D)dt \tag{5}$$

where I is the ionic current in the electrode. During the discharging process using the zero-voltage approach, the stored energy is released in the CDI cell and is carried out of the system via the ionic species. Therefore, the ratio of the $E_{stored,total}$, and E_{used} of each system yields the maximum energy recovery, ER, that can be theoretically achieved.

Beside the efficacy of each CDI system in recovering part of the expended electrical energy for desalination, energy efficiency of the system in removing the species from the saline feed can be determined. For this purpose, thermodynamic efficiency, η, defined as the ratio of the minimum required work for desalination to the actual energy consumption is calculated. Regardless of the desalination method, the minimum work required to divide a solution into two less concentrated and brine fractions, under ideal reversible conditions can be derived from the Gibbs free energy and be stated as follows [32,67]:

$$W_{rev} = 2V_d\left(\frac{c_o}{WR}ln\frac{c_o - WR.\,c_d}{c_o} - 2c_d ln\frac{c_o - WR.\,c_d}{c_d(1-WR)}\right) \tag{6}$$

where, V_d, c_o, and c_d are the desalinated volume, initial salinity, and the final concentration of the desalinated solution, respectively. WR is the water ratio which is the volume ratio of the desalinated and initial stream. Based on Eqs. (4)–(6), the thermodynamic efficiency of the CDI system is calculated as:

$$\eta = \frac{W_{rev}}{E_{\text{used}}} \tag{7}$$

2.3. The performance evaluation criteria and figure-of-merit

It should be noted that lower concentration of the solution at the exit does not necessarily define an efficient and effective desalination process. Reaching 1% of the initial concentration may be an indication of a desirable system at the first glance. Yet achieving such outcome for two liters of solution in one day does not seem satisfactory. For electrodes with the same geometry, the minimum concentration is reached faster at higher flow rates [41,47]. Additionally, in a certain period of time, higher flow rates lead to higher volumes of the desalinated water. Larger volumes of water treated in a shorter amount of time alleviate lower desalination percentage obtained in developing systems with

high flow rates. As such, an inclusive metric is needed to make a complete assessment of the desalination performance in different CDI systems, considering the trade-offs between the aspects of the final outcome.

In addition to low minimum average concentration of the effluent, fast ion adsorption from large volumes of water is favorable in a desalination unit. We combine these characteristics into a new figure-of merit, called *Ultimate Desalination Throughput (UDT)*:

$$UDT = \frac{(c_0 - c_{ave,min})}{c_0}((c_0 - c_{ave,min})\, Q_{\text{desal}})\,(t_{ave,min}\, Q) \tag{8}$$

where $t_{ave,min}$ is the instant of time when minimum average concentration is reached, and Q is the flow rate in the system. Q_{desal} is flow rate of the desalinated water which is defined as the ratio of the desalinated volume and the total desalination time. For a one-cycle desalination system, this value is the same as the Q, whereas they are different in multi-cycle arrangements, where the desalinated volume is volume of the treated water in the last cycle. The first term in Eq. (8) determines the desalination percentage in the system, while the second term is associated with the rate at which salts are removed from the feeding solution. The last term indicates total volume of the water treated until the minimum average concentration is achieved at the exit. For a one-cycle CDI arrangement, *UDT* is equivalent to product of the amount of adsorbed salt and the rate of adsorption. This is akin to the conceptual diagram proposed by Kim and Yoon which plots *ASAR* against *SAC* to evaluate CDI performance [17]. According to this diagram, an optimum is reached when the product of the two metrics is maximum.

In addition to the desalination process, performance of the regeneration stage should be considered to make a thorough assessment of the overall performance of a CDI system. The less water is used for regenerating the electrodes, the more efficient the systems is in terms of water consumption. Desalinating 1 l of brackish water, while employing 50 l to discharge the electrodes deteriorates the efficacy of the system. Moreover, in a certain period, shorter regenerations enable more desalination cycles to be conducted and therefore, higher volumes of water to be treated. Therefore, in conjunction with high values of *UDT,* high water recovery ratios (*WR*), defined as volume of the desalinated water over total volume of the consumed water, as well as short total processing time (desalination and regeneration) are crucial for an efficient CDI system. We integrate all the mentioned characteristics and propose another metric which is referred to as the *Overall Desalination and Regeneration Performance (ODRP)*:

$$ODRP = UDT\frac{WR}{t_{total}} \tag{9}$$

where, t_{total} is the time of desalination and regeneration combined.

It should be noted that while *UDT* allows for an inclusive comparison between desalination performance of different systems, *ODRP* considers the overall performance of the CDI configuration including both the desalination and regeneration stages. Furthermore, the proposed figure-of-merits can be employed to measure multi-cycle systems against single-cycle arrangements. To desalinate a specific solution up to a target concentration, water can go through one fully-developed cycle flowing at a relatively low flow rate, or multiple consecutive developing cycles at higher flow rate. Even though each cycle of the latter approach results in lower desalination percentage than the former, the processing time at each stage of the developing regime is lower than the fully developed one. *UDT* and *ODRP* are thus, appropriate and practical means to evaluate the inherent trade-offs associated with such systems.

3. Method

All the numerical analyses are performed in COMSOL Multiphysics 4.2 using a 50 × 10 mm symmetric CDI cell. In addition to being dimensionally comparable to the experimental CDI units in literature, this cell size allows for implementing a large number of computationally efficient simulations [23,57,68]. The cell comprised of one pair of porous electrodes, with a total porosity of 0.7, volumetric micropore capacity of 0.15 GF/m^3 (adopted from the previous work by Hemmatifar et al. [46]), and tortuosity of 1. At each side of the main channel, electrodes are pressed against the current collectors with no contact resistance. All the desalinations and regenerations are conducted at 1 V and zero voltage, respectively, assuming no external electrical resistance. As mentioned before, the mD model includes a non-electrostatic adsorption term to account for adsorption of the ions prior to applying the electrical voltage. Although, some studies assume a constant value for this parameter [23], this term may change with concentration in micropores and over time [23,39]. However, in this work, the focus is directed towards the electro-sorption of the ions in the porous media and its effect on the concentration profile at the exit of the system. Hence, we disregard the non-electrostatic adsorption term in the 2D model. In addition, it was assumed that all the main channel and porous media are initially filled with the feeding solution. Preliminary numerical results are compared with the previous works in the literature to validate the model by considering similar configurations. For each set of simulations, mesh size and time step independencies along with the conservation of mass and energy are confirmed.

3.1. Transport phenomena in CDI

To investigate the interplay between the transport mechanisms in the bulk flow and in the porous electrodes, full desalination and regeneration CDI experiments are simulated under conditions where the whole process is limited by either the bulk advection, bulk diffusion, or microscale electro-diffusion. Fig. 3 presents the map of non-dimensional numbers and the table of timescales associated with each of the desalination/regeneration cases considered in this study. 6 CDI simulations are conducted with combinations of different timescales. In each case, one of the mechanisms has the largest timescale (being the slowest among them), one of the mechanisms features a timescale that is one order of magnitude lower than the largest one, and the last mechanism is the fastest with a timescale two orders of magnitude lower than that of the slowest one. Furthermore, 6 sets of full desalination and regeneration cycles are simulated in which two of the transport mechanisms take place at the same rate. While these two mechanisms have the same order of magnitude time constants, the third mechanism is one order of magnitude slower or faster. Finally, a full desalination/regeneration simulation is related to the case where all the three transport phenomena have timescales of the same order. Timescales related to the bulk advection, bulk diffusion, and microscale electro-diffusion are changed by manipulating the flowrate, electrodes' gap distance, and thickness of the electrodes. The initial salinity for all these 13 cases are the same and is set as 8.8 mg/ml (equal to 150 mM), which is in the lower range of brackish water and is typically applicable to CDI systems [39]. The same solution is used for regenerating the electrodes and the regeneration stage is carried out by adopting the zero-voltage approach.

3.2. Regeneration schemes in the multi-cycle CDI systems

The desalination/regeneration cases analyzed in the previous section go through successive simulations to replicate desalinating a solution with a set salinity for several times in a single CDI cell, under the multi-cycle configuration. As it was stated in Section 2.2, to achieve a solution with lower concentration than what can be desalinated in 1 cycle, each desalination cycle operates until the average concentration at the exit reaches its minimum value. The average concentration is calculated using Eq. (3). Subsequently, the inlet concentration of each cycle is set as the minimum average concentration of the effluent in the previous one. To regenerate the porous electrodes, three different scenarios are explored. Fig. 4 illustrates concept of the proposed

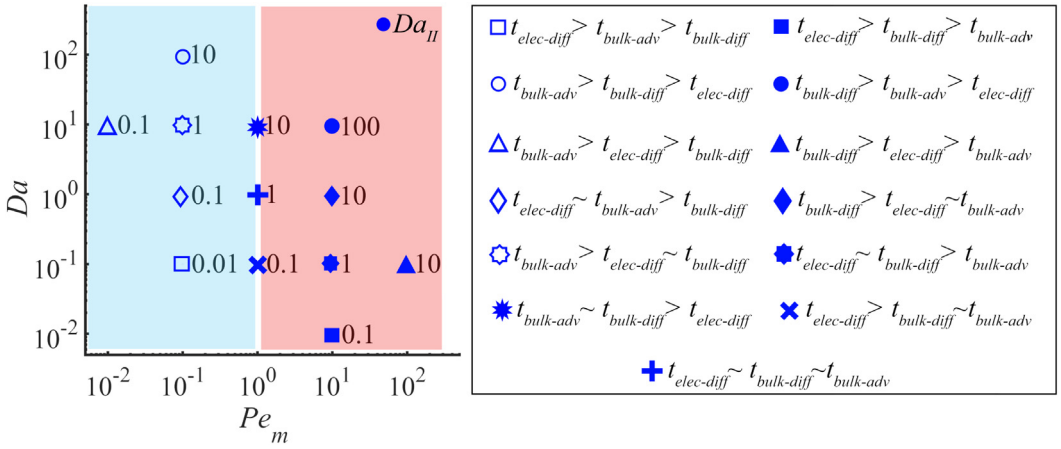

Fig. 3. Non-dimensional numbers (left) and timescales (right) of the simulated cases. In the graph, numbers next to the points represent the Da_{II} associated with each case. Blue and red regions illustrate fully developed and developing regimes, respectively. (For interpretation of the references to color in this figure legend, the reader is referred to the web version of this article.)

regeneration schemes in a multi-cycle CDI arrangement with the initial concentration of c_0 (which is intended to decrease through this multi-cycle configuration). To better illustrate the concept of the regeneration schemes, the desalination stage at the i-th cycle with the effluent of $c_{D,i}$ (which is the minimum average concentration obtained at the exit) is depicted in Fig. 4.a. This solution is set as the inlet of the desalination stage of the next cycle (Fig. 4.b). After reaching the minimum average concentration in the $i+1$-th cycle ($c_{D,i+1}$), the cell proceeds to the regeneration stage. In the first regeneration scenario (Fig. 4.c), the cell is discharged using the initial main solution (c_0), and the same approach is applied for all the regeneration stages. In the second regeneration approach (Fig. 4.d), the regenerating feed stream is brine of the previous cycle ($c_{R,i}$). In this scenario, at each cycle the brine collected at the end of the previous cycle is used to discharge the electrodes. In the third regeneration scheme (Fig. 4.e), at each cycle both desalination and regeneration processes use the same feed solution ($c_{D,i}$). In other words, effluent of each desalination stage serves as the influent of the desalination and regeneration of the next cycle To prevent re-salination of the desalinated water inside the cell during the discharging process and to avoid mixing of the regeneration feed stream with the desalinated solution in the unit, some groups have suggested a rapid flushing step between each desalination and regeneration step in multi-cycle arrangements [69,70]. However, following typical multi-cycle CDI systems [13,20,71,72], in this work we perform all the regeneration steps immediately after the desalination stages without any flushing step. In all the scenarios, prior to each charging stage, the cell is flushed with the desalination feed stream until the concentration at the exit is equal to the inlet concentration.

Initial concentration in most of the cyclic cases is set to 5 mg/ml although the initial solution in some of the cases has a different salinity. Cases with very fast electro-diffusion in the electrodes and slow bulk advection experiences near zero concentration in the macropores due to an extreme concentration depletion, known as electrode starvation. The very slow advection fails to provide the ionic species sufficiently fast for further adsorption in the porous media, leading to zero-concentration macropores for a substantial amount of time, which leads to computational complications in the simulations. Therefore, for these specific cases, the first cycle starts with higher salinity solutions (8–15 mg/ml),

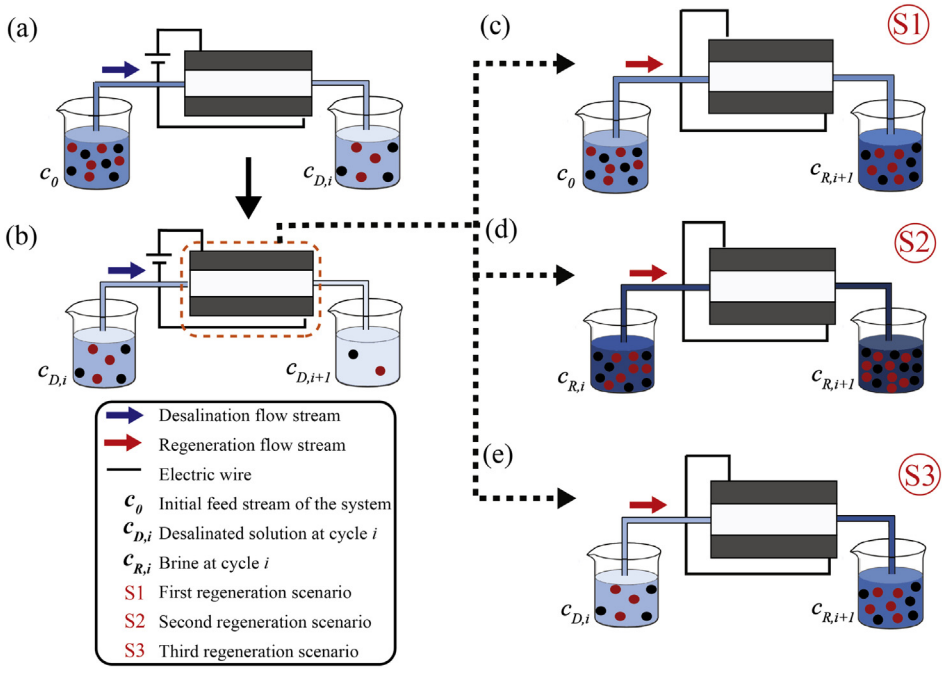

Fig. 4. Schematic illustration of the proposed discharging schemes in a multi-cycle arrangement with the initial concentration of c_0. (a) The i-th desalination stage which continues until the minimum average concentration ($c_{D,i}$) is reached at the exit. (b) The $i+1$-th desalination stage where the minimum average concentration of the effluent is $c_{D,i+1}$. Three scenarios are proposed to discharge the electrodes (S1, S2, and S3), each differing in the regeneration feed stream. (c) S1: The main reservoir of the system, c_0, is used for the regeneration. (b) S2: Brine of the previous cycle, $c_{R,i}$, is utilized to discharge the electrodes. (d) S3: The electrodes are regenerated using the influent of the desalination stage, $c_{D,i}$. (same solution is used for both desalination and regeneration at each cycle).

still within the range of brackish water (0.5–35 mg/ml). However, it should be noted that due to the comprehensive nature of the characterization metrics proposed in Section 2.3, one is able to evaluate performance of CDI systems even with different initial concentrations.

Regeneration of the electrodes effectively takes place until a zero-charge state is reached. In real-life experiments, this can be determined by measuring the electrical current passing through the electrodes which decays to zero once the zero-charge state is achieved. However, this stage does not necessarily guarantee the complete removal of desorbed ions from the CDI cell, as they need to diffuse through the electrode and the main channel and finally exit the cell via the flow stream. If the desorbed ionic species are not entirely removed from the cell, at the desalination stage of the next cycle they will be re-adsorbed into the micropores. Therefore, less of the electrodes' capacity is devoted to removal of species entering the cell through the desalination feed stream. To simulate realistic experimental procedures, in this work the discharging process continue until the concentration at the exit of the cell is equal to that in the regeneration feed stream. *UDT*, *ODRP*, *ER*, and η are used to evaluate desalination and regeneration efficiency of the cyclic CDI systems using the proposed regeneration schemes.

4. Results and discussion

Here, first we present the results of the parametric study on effects of the interactions between the bulk and porous electrode transport phenomena on the output profile concentration of the CDI cell. Then, we evaluate the performance of the discussed regenerations schemes in successive multi-cycle CDI systems.

4.1. Parametric study of transport phenomena in CDI

Fig. 5 shows the effluent concentration profile for the six cases with different permutation of the characteristic timescales (the reader is referred to Fig. S1 in the supplementary document for the other studied cases). From Fig. 5 and Fig. S1, a direct correlation can be inferred between the time that the minimum concentration is achieved (t_{min}) and the $t_{bulk\text{-}adv}$. In all the cases, t_{min} is in the same order of magnitude as $t_{bulk\text{-}adv}$ which means in each system it takes about $t = t_{bulk\text{-}adv}$ to reach the bulk flow advective-diffusive “steady state”. This “steady state” refers to the period when the outlet concentration is at its minimum value. After application of the electrical voltage, all the ions in the main channel experience a diffusion towards the porous electrodes because of the concentration depletion in the electrode, and an advection through the main channel due to the flow of the stream. Concentration decreases as long as the number of ions removed from the main stream through diffusion is increasing (comparing to the previous time step). For any ion entering the cell, if the bulk diffusion fails to remove the ion from the main stream, on average it takes about one advection time constant to leave it (although this would take slightly longer than the $t_{bulk\text{-}adv}$ as the ion's path is shifted due to the bulk diffusion). On average, ions entering the cell afterwards will undergo the same process. At this point, the system reaches its maximum capacity to decrease the concentration of the feeding solution, leading to the minimum concentration at the exit. Depending on the rate of the advection in the unit, this state lasts for a relatively short (small $t_{bulk\text{-}adv}$) or long (large $t_{bulk\text{-}adv}$) time. This has also been experimentally verified, as in numerous studies t_{min} is shown to be affected by the flow rate in the stream which directly changes the $t_{bulk\text{-}adv}$, and unaltered by the initial concentration which affects the $t_{elec\text{-}diff}$ [41,46,73].

Analyzing the concentration profile at the exit of the CDI units with different timescales also reveals a sudden and sharp change in the saturation rate in the electro-diffusion limiting systems (inset of the effluent concentration profiles in Cases 1 and 2 in Fig. 5). As mentioned before, the concentration depletion in the macropores of the porous media leads to the diffusion of species from the main channel into the electrodes. Subsequently, removal of salt species from the main solution via bulk diffusion leads to concentration reduction at the outlet. Large values of $t_{elec\text{-}diff}$ (slow electrodes' charging process) indicate slow spread of the concentration depletion and the subsequent diffusion in the electrodes whereas the bulk diffusion and advection in the main

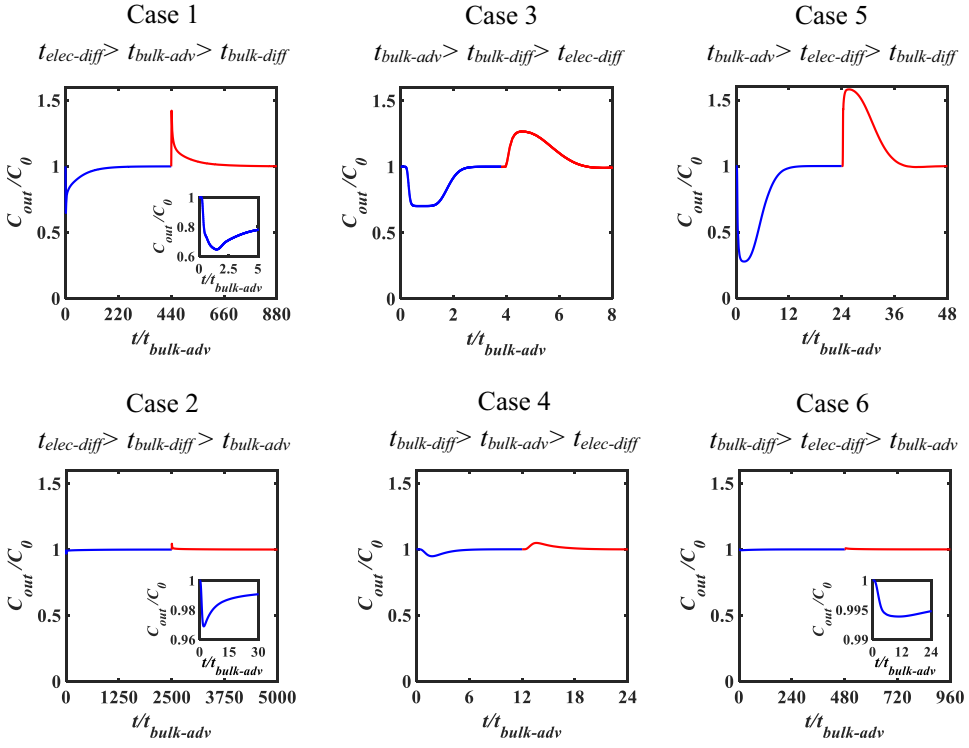

Fig. 5. Normalized concentration profile at the exit of CDI systems operating with different permutation of characteristic timescales and same initial concentration. Time is normalized by the advection timescale in each case.

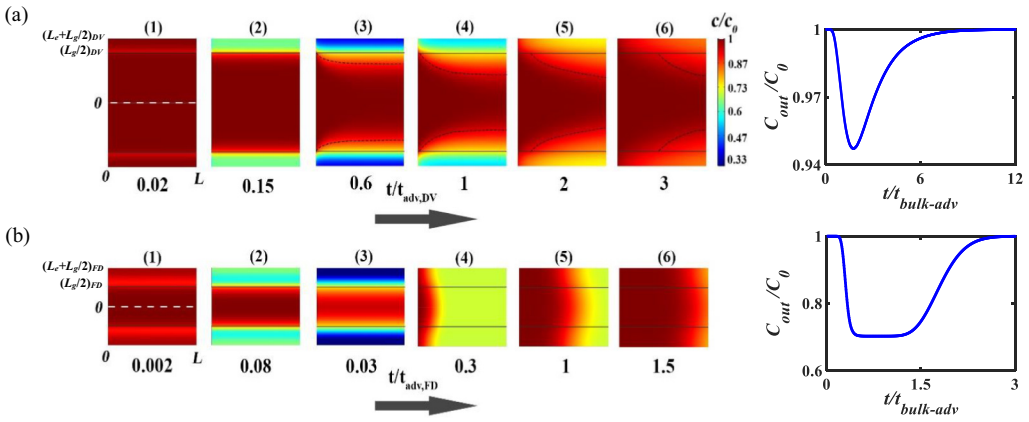

Fig. 6. Normalized concentration in (a) developing (DV), and (b) fully developed (FD) regimes at different time steps. On the right, concentration of the effluent and on the left, salt concentration in the macropores and main channel of the cell (not-to-scale) are presented for each regime (white dashed lines illustrate centerline of the cells, and the solid black lines are the interface between the electrodes and the bulk flow). Both regimes experience a concentration depletion shortly after applying the electric voltage. After that, a concentration shock-wave appears in the system due to the coupling of macro- and microscale transport mechanisms. In the developing regime, the whole process is limited by the slow diffusion in the main channel towards the electrode, therefore the wave spreads in a relatively upward direction. Black dashed lines depict the growing convective-diffusive layer inherent with a developing system, at which the mass transport towards the electrode is more significant than the advection of species within the bulk flow. On the contrary, in a fully developed regime, the shock-wave propagates rather longitudinally, in direction of the slow advection which limits the whole charging process. This phenomenon results in an "infinite capacity" where the effluent concentration remains at its minimum value for a relatively long time. In this system, the convective-diffusive layer is not detectable as bulk diffusion of the species in the main channel towards the porous media is uniform at each cross section.

channel take place at faster rates. Consequently, in electro-diffusion limited systems, slow motion of the ions within the porous media does not meet the speed of the species entering the electrode. This renders the bulk diffusion incapable of further salt removal from the main channel after the initial drop in the outlet concentration. Therefore, the concentration of the effluent reaches its minimum value before the concentration depletion happens everywhere in the porous electrode. Eventually, following the concentration depletion occurring in the entire electrode, slow microscale diffusion effectively takes place in all the macropores. This phenomenon leads to a decrease in the saturation rate of the porous electrodes which can be noticed in the concentration profile at the exit of the cell.

To get a better understanding of the concentration behavior at the exit of different cases, we also analyze the concentration in the main channel and in the electrodes for two cases of developing and fully developed conditions under the same rate of electro-diffusion. Fig. 6.a and Fig. 6.b show normalized concentration in the cell at different time steps after applying the electric voltage, in a developing ($t_{elec\text{-}diff} < t_{bulk\text{-}adv} < t_{bulk\text{-}diff}$) and fully developed ($t_{elec\text{-}diff} < t_{bulk\text{-}diff} < t_{bulk\text{-}adv}$) regimes with fast electro-diffusion, respectively. Concentration distribution in the main channel as well as in the electrodes are shown using a color scheme. The concentration at the exit of the CDI cell is also plotted for the developing and fully developed regimes. Shortly after applying the voltage, due to the quick and simultaneous attraction of counter-ions and repulsion of co-ions in the micropores, both developing and fully developed systems experience a concentration depletion, near the interface of the electrodes and the main channel (Fig. 6.a.1 and b.1). Note that since in these systems the capacity of the microporous electrode is greater than the population of ionic species that are initially present in the system, this concentration depletion does not lead to starvation of the macropores, which happens when locally $c_{ma} \approx 0$. Because of the fast electro-diffusion of the ionic species in these two systems, the emerged concentration depletion in the electrodes spreads in the inward direction at a rapid rate (Fig. 6.a.2–3 and b.2–3). Nevertheless, the micropores need to wait for the bulk advection and diffusion to receive ions from the solution. This interplay of the micro- and macroscale transport mechanisms results in propagation of a concentration shock-wave through the unit which can be seen in both regimes (Fig. 6.a.4–6 and b.4–6). Previous research in this regard mainly focused on CDI systems with slow microscale diffusion in the electrodes (electro-diffusion limited), and did not investigate the shock-wave in units with different limiting transport mechanisms. Despite the fast advection in the diffusion limited regime (Fig. 6.a), micropores need to wait for the ionic species to diffuse into the electrodes and get adsorbed into the surface of the electrode. In other words, the slow bulk diffusion hinders the whole adsorption process. Therefore, the shock-wave propagates mainly in the direction of the bulk diffusion across the gap. Nevertheless, in an advection limiting system (Fig. 6.b), this concentration wave spreads rather longitudinally. In such system, although the species are transported into and within the electrode at a higher rate owing to the faster bulk diffusion and microscale electro-diffusion, the micropores are forced to wait for the slow advection in the main stream to deliver the species to the electrode. Thus, the concentration shock-wave spreads in the direction of the advection along the cell.

In the fully developed systems where the whole process is limited by the slow advection, the low concentration region formed in front of the shock-wave moves slowly along the main channel. This leads to the effluent concentration staying at the minimum level for an extended period of time, akin to having an infinite capacity in the cell. Such behavior of infinite capacity has been previously reported in experimental data as well [41].

After the initial concentration depletion of the macropores in the electrodes (Fig. 6.a.3), the growing convective-diffusive layer can be observed in the developing system (marked with the black dashed lines in the colored computational unit). As it is illustrated, in the developing system the bulk diffusion of the species towards the electrodes mainly happens in the thin convective-diffusive layer close to the interface of the electrodes and the bulk flow. However, this sub-region cannot be seen in the fully developed regime, presented in Fig. 6.b. In this regime, at each transverse cross section the concentration gradient normal to the flow stream is lower than that in the developing system.

4.2. Regeneration schemes for multi-cycle CDI arrangements

In this section, we investigate the performance of CDI systems presented in Fig. 5, in a cyclic arrangement. Each desalination is conducted until the minimum average concentration is achieved at the exit. The electrodes are then discharged, adopting three different regeneration scenarios described in Fig. 4, where in the first scenario (S1) the same feeding reservoir is used to discharge the electrodes in each cycle meaning that concentration of the regeneration solution is constant and equal to the initial concentration of the system for all the cycles. In the second scenario (S2) each cycle is regenerated using the brine from the previous cycle. In the last regeneration scenario (S3) the same solution is used for both desalination and regeneration at each cycle. We use

Table 1
Performance evaluation of fully developed and developing CDI systems with different rates of electro-diffusion, in 1 cycle of desalination and regeneration. Systems are compared in terms of desalination efficacy, overall performance, energy recovery and thermodynamic efficiency. Gray and white rows represent fully developed and developing regimes, respectively.

Case	UDT ($\frac{mM.ml}{s}$)×10^5	ODRP ($\frac{mM.ml}{s^2}$)×10^9	ER (%)	η (%)
$t_{elec\text{-}diff}$>$t_{bulk\text{-}adv}$>$t_{bulk\text{-}diff}$	0.74	3.93	30.61	0.14
$t_{elec\text{-}diff}$>$t_{bulk\text{-}diff}$>$t_{bulk\text{-}adv}$	1.50	270.22	26.59	0.04
$t_{bulk\text{-}adv}$>$t_{bulk\text{-}diff}$>$t_{elec\text{-}diff}$	0.15	0.32	52.86	0.39
$t_{bulk\text{-}diff}$>$t_{bulk\text{-}adv}$>$t_{elec\text{-}diff}$	0.97	25.90	52.54	0.11
$t_{bulk\text{-}adv}$>$t_{elec\text{-}diff}$>$t_{bulk\text{-}diff}$	0.99	1.40	58.23	6.17
$t_{bulk\text{-}diff}$>$t_{elec\text{-}diff}$>$t_{bulk\text{-}adv}$	3.32	202.17	44.70	0.04

UDT and *ODRP* along with the energy recovery ratio and thermodynamic efficiency to compare efficacy of these scenarios.

Table 1 compares the performance of the developing and fully developed regimes with the same rate of electro-diffusion in the first cycle. In the fully developed convective-diffusive regimes, slow advection in the unit provides species with more time to be effectively diffused towards the interface of the electrode and the bulk flow compared to the developing regimes with faster bulk advection and slower bulk diffusion. Therefore, with the same rate of electro-diffusion in the electrodes, fully developed systems reach lower minimum concentrations than the developing systems. The apparent superiority of fully developed regimes over developing for achieving higher desalination percentage, which is evident from the plots in Fig. 5 and Fig. S1, has also been extensively investigated in the literature where reducing the flow rate decreases the minimum concentration of the effluent [34,41,47]. Nevertheless, interpreted from comparison of the *UDT*s, CDI cells with developing regimes show a better desalination performance than fully developed ones. Although at first it may appear that the fully-developed systems have better desalination capacity due to higher levels of desalination that can be achieved, developing regimes deliver preferable performance as they desalinate more volume of initial solution in a shorter amount of time. Moreover, as it can be seen in Table 1 thanks to the faster desalination and regeneration of the developing regimes, each CDI cycle in such systems is shorter than their counter-system with the same $t_{elec\text{-}diff}$. This along with higher *UDT* translates into higher *ODRP* in these systems. To completely exploit the short developing cycles, water can be desalinated in a developing multi-cycle arrangement rather than a fully developed single-cycle one. In other words, to desalinate a given solution up to a particular concentration, it can be treated through multiple short cycles operating at a developing regime instead of one long, fully developed cycle. Although the latter delivers higher desalination percentage in 1 cycle, as it is shown, shorter developing cycles results in better overall performance.

Here, we also evaluate the energetic performance of the CDI units with different characteristic time constants. As it can be seen from the data shown in Table 1, for similar electro-diffusion time constant in the first cycle, contrary to their desalination performance, developing regimes offer lower energy recovery ratio as well as thermodynamic efficiency than the fully developed configurations. The lower energy efficiency of the developing regimes has also been experimentally investigated by Zhao et al. where they showed that energy consumption per ion removed increases by increasing the flow rate in the system [27]. Higher levels of desalination obtained in the fully developed regime result in higher energy storage which subsequently enhance the ability of the cell to recover part of the used energy for the desalination process. Additionally, for a certain solution, higher values of the minimum work are required to reach lower outlet concentrations (see Eq. (6)). This makes the CDI process to be more energetically justifiable. Hence, because of their inherent higher levels of desalination, fully developed regimes are thermodynamically more efficient than developing systems.

Fig. 7 presents the desalination and energetic efficiency of the proposed discharging scenarios in a cyclic arrangement. The overall increase of the *UDT* with the number of desalination cycles proves the effectivity of the proposed multi-cycle arrangement in improving the desalination performance of the CDI systems. As the initial solution goes through more cycles, it gets desalinated to lower salinity levels which has an increasing effect on the overall desalination percentage and therefore, on the value of *UDT*. Further analysis of the proposed multi-cycle arrangements reveals that in these systems, the overall adsorption rate generally decreases with the number of desalination cycles (data not shown here). However, in some cases this rate increases after reaching a minimum value. Several research groups have investigated the salt adsorption rate in different CDI systems [15,47,74]. Zhao et al. showed that the removal rate depends on different parameters of the CDI system, including the initial concentration, flow rate, and desalination time [47]. Keeping all the other parameters of a system constant, their experimental and theoretical data showed that the rate of adsorption reaches a maximum value by varying either the adsorption time or the initial concentration, at a time. In the present work, since both of these parameters change from 1 cycle to another, it is not evident how they impact the overall adsorption rate. The general increasing trend in the value of *UDT* implies that in most cases the increase in the overall desalination percentage associated with running more desalination cycles exceeds the decrease in the corresponding adsorption rate. Nevertheless, in cases with very slow diffusion in the bulk flow, the reduction in the salt removal rate surpasses the increase in the desalination percentage after a few desalination cycles, resulting in an optimum number of cycles with the highest *UDT*. Moreover, the data show that in the systems with fully developed conditions, the desalination performance does not depend on the regeneration scenario. Regardless of the discharging scheme, the value of *UDT* in these systems is the same for all the regeneration scenarios and increases with the number of desalination cycles. During each cycle for these systems, the relatively fast bulk diffusion enables the CDI cell to get completely cleaned from the previous regeneration feed solution at the priming step, and therefore, minimized the effect of the regeneration approach on the desalination performance.

As it can also be inferred from the plots in Fig. 7, by increasing the number of cycles *ODRP* drops substantially in all the cases. Longer processes and lower water recovery ratios are the main reasons for the considerable decline in the efficacy of the systems through more cycles. As explained earlier, before desalination takes place at each cycle, the cell is primed with the desalination feed stream. Therefore, to have enough solution for the desalination and priming stages, the preceding cycle should be operated several times. This exponentially increases the total number of times that all the previous cycles are required to run which substantially extends the total duration of the overall process and decreases the water recovery ratio. For example, assume a three-cycle system. One should run more than one, let's say N_2 number of cycle 2 to provide enough solution for priming and desalinating steps in the third cycle. This leads to N_1 number of the first cycle such that the second

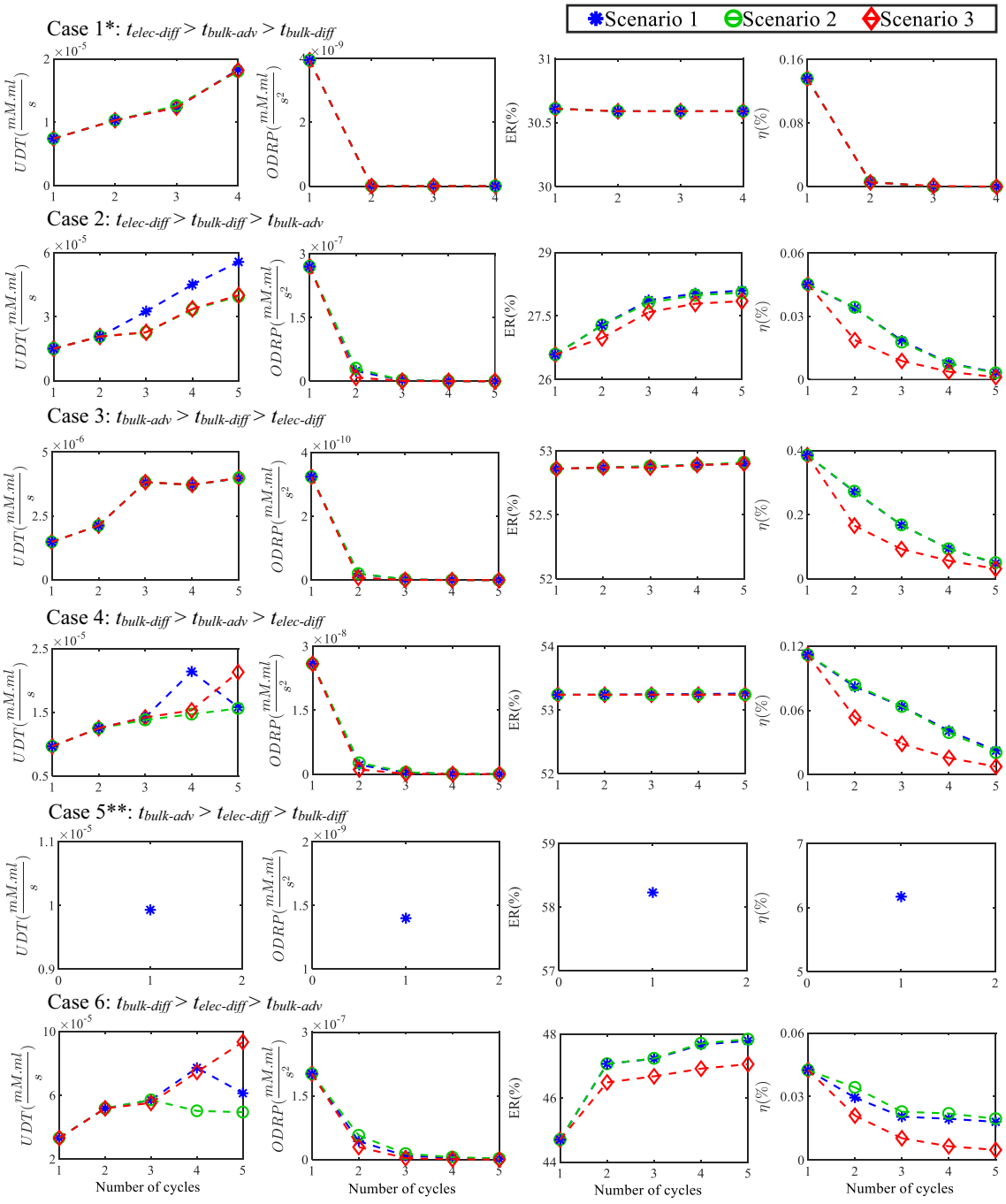

Fig. 7. Efficacy of CDI systems operating with different limiting transport mechanisms, in terms of desalination, overall performance, energy recovery, and thermodynamic efficiency. The x-axis shows the number of desalination cycles.

*In this system, the effluent concentration reached below the lower bound of brackish water (0.41 mg/ml) after 4 cycles, in all the regeneration schemes.

**In this case, with the 5 mg/ml inlet stream, the average concentration of 0.42 mg/ml (below the criterion for brackish water) is obtained at the exit after only 1 cycle.

cycle will have sufficient volume of inlet solution to perform for N_2 cycles, where N_1 is clearly greater than N_2. Now, if one more cycle is added to the arrangement, the third cycle needs to operate more than once to produce enough feed solution for the priming and desalination stages of the next cycle. Subsequently, the second and first cycles must desalinate/regenerate for N_2' and N_1' times, respectively, where obviously $N_1' > N_1$ and $N_2' > N_2$. Adding another cycle to a multi-cycle CDI system not only increases the total operation time of the previous cycle but it also affects the processing time in all the earlier cycles, resulting in a significant rise in the duration of the whole process and volume of the consumed water. Therefore, as the number of cycle increases, the overall performance of the system diminishes even though their desalination performance generally increases. It is worth mentioning that this effect is more noticeable in the third scenario where the same influent is utilized for priming, desalinating and regenerating at each stage. It can be concluded from the plots that due to the intrinsic higher water recovery ratios in the second discharging scenario, S2 has slightly better overall performance (*ODRP*) among all the three regeneration schemes.

Energetic performance of the investigated cases is also depicted in

Fig. 7. The overall energy recovery ratios calculated for these cases express an either constant or increasing behavior with the number of cycles. In the cases where the bulk advection is not a fast mechanism, the time required to prime the CDI unit before each desalination cycle is very long. In other words, due to the relatively slow advection in the main channel it takes a long time for the concentration at the outlet to reach its value in the inlet stream. In such systems, each cycle should be operated for considerably large number of times to provide enough inlet solution for the long priming stages of the following cycles. In these cases, the solution should go through the first cycle so many times that most of the total energy is consumed and recovered in this cycle, and therefore, the overall energy recovery ratio in the subsequent cycles only slightly changes relative to its value in the first cycle. Conversely, in cases with fast advection in the main channel, the outlet concentration quickly reaches the inlet concentration and the cell is discharged and primed very fast. It should be noted that even at the end of the priming stage, the electrodes are not necessarily filled with the desalination feed stream and the ionic species left from the previous cycle may remain in the electrode. This is more noticeable in the systems with fast advection in the bulk where the electrodes cannot effectively get cleaned prior to each desalination step due to the slow electro-diffusion and bulk diffusion in the system. This higher left-over concentration in the electrodes reduces the ionic resistance in the system and boosts the energy recovery, as it can be seen in Fig. 7. Since the concentration of the regeneration feed stream in the third scheme is lower than the other two scenarios, lower energy recoveries are obtained in this scheme. These results are in agreement with the work by García-Quismondo et al. as they have shown that increasing the concentration in the CDI unit enhances the energy recovery ratio [63]. In another work, Zhang et al. used a constant-current system and also showed that discharging the electrodes with higher salinity solutions improves the energy recovery [64].

Although the overall desalination percentage and the number of adsorbed ions increase by performing multiple consecutive cycles, the thermodynamic efficiency decreases as the system consumes more energy, resulting in a trade-off between the desalination performance and the energy efficiency of the CDI systems. This drop in the energy efficiency is more significant in the third regeneration scheme. Considering larger total number of times each cycle should be repeated in S3 comparing to S1 and S2, higher values of energy are utilized in this scenario. It should be noted that even though the thermodynamic efficiencies of the systems in this parametric study are noticeably low ($< 10\%$) the results are consistent with previous experimental data [4,26]. The primary reason for the substantial difference between the energy consumption and the reversible work of desalination in the simulations is the ionic resistivity of the solutions. As it was mentioned before, in the CDI cell, which from an electrical standpoint can be considered as a combination of the capacitors and resistors, the energy loss is due to the resistivity in the system. In other words, the resistivity of the ionic solutions in the bulk flow and porous electrodes leads to energy inefficiency in the system. Although the initial concentration in this set of simulations are in the range of brackish water, the electric resistivity of the inlet streams is at the order of 100 Ω·m. These initial solutions with relatively low conductivity result in energetically inefficient desalination systems.

5. Conclusion

In this work, we conducted a parametric study on CDI systems to investigate the interplay between micro- and macroscale transport mechanisms and its effect on the overall performance of these systems. By permutation of the time constants associated with each mechanism, desalination efficacy and energy efficiency of different desalination cells were investigated. To achieve a comprehensive analysis of CDI units, we introduced inclusive metrics which encompass different aspects of an effective desalination system. Mainly, we focused on comparing developing convective-diffusive regimes with fully developed ones that can be obtained at higher and lower flow rates, respectively. Despite the superiority of the former in terms of desalination performance, the latter showed higher values of energy recovery and thermodynamic efficiency. Additionally, to further decrease the concentration of a given ionic solution, multi-cycle arrangements were proposed and simulated, in which minimum average concentration achieved at the exit of each cycle was set as the inlet concentration of the following one. To reach higher levels of desalination percentage and water recovery ratio, three regeneration schemes were introduced, each of which employed different feed streams for discharging the electrodes. Simulating different cyclic CDI configurations indicated a trade-off between desalination and energetic performance. While better desalination performance (in terms of desalination percentage, volume of treated water and rate of ion removal) could be generally achieved by desalinating through multiple consecutive cycles, it led to thermodynamically inefficient systems. This energy inefficiency was more evident in CDI systems where desalination effluent of each cycle was utilized as both the desalination and regeneration inlet streams of the next cycle. Utilizing the brine collected at the end of the regeneration stage of each cycle as the regeneration feed stream of the following cycle resulted in better overall performances (in terms of desalination, water recovery ratio and total duration of the process). This study provides deeper insights of the effects of the coupling between the multiscale transport phenomena in CDI on the effluent of the system. Moreover, these findings allow for better guidelines on design and implementation of efficient CDI systems with improved overall performance in different applications.

Acknowledgment

The authors would like to thank Ali Hemmatifar for his help in the initial implementation of the COMSOL simulations and Pooyan Tirandazi for fruitful discussions. This work was funded by Northeastern University start-up funds.

Appendix A. Supplementary data

Supplementary data to this article can be found online at https://doi.org/10.1016/j.desal.2018.03.022.

References

[1] WWAP, The United Nations World Water Development Report 2015: Water for a Sustainable World, UNESCO, Paris, France, 2015.
[2] (Programme) WUNWWA, Wastewater: the untapped resource, The United Nations World Water Development Report 2017, UNESCO, Paris, 2017.
[3] J. McGlade, B. Werner, M. Young, M. Matlock, D. Jefferies, G. Sonnemann, M. Aldaya, S. Pfister, M. Berger, C. Farell, et al., Measuring Water Use in a Green Economy, UNEP, 2012.
[4] O.N. Demirer, R.M. Naylor, C.A.R. Perez, E. Wilkes, C. Hidrovo, Energetic performance optimization of a capacitive deionization system operating with transient cycles and brackish water, Desalination 314 (2013) 130–138.
[5] M.A. Anderson, A.L. Cudero, J. Palma, Capacitive deionization as an electrochemical means of saving energy and delivering clean water. Comparison to present desalination practices: will it compete? Electrochim. Acta 55 (12) (2010) 3845–3856.
[6] Y. Salamat, C.A. Rios Perez, C. Hidrovo, Performance characterization of a capacitive deionization water desalination system with an intermediate solution and low salinity water, J. Energy Resour. Technol. 138 (3) (2016) 032003.
[7] Y. Salamat, C.A. Rios Perez, C. Hidrovo, Performance improvement of capacitive deionization for water desalination using a multistep buffered approach, J. Energy Resour. Technol. 139 (3) (2016) 032003.
[8] J.F. Klausner, Y. Li, M. Darwish, R. Mei, Innovative diffusion driven desalination process, J. Energy Resour. Technol. 126 (3) (2004) 219–225.
[9] M. Shatat, M. Worall, S. Riffat, Opportunities for solar water desalination worldwide: review, Sustain. Cities Soc. 9 (2013) 67–80.
[10] N. Ghaffour, J. Bundschuh, H. Mahmoudi, M.F.A. Goosen, Renewable energy-driven desalination technologies: a comprehensive review on challenges and potential applications of integrated systems, Desalination 356 (2015) 94–114.
[11] Y. Oren, Capacitive deionization (CDI) for desalination and water treatment — past, present and future (a review), Desalination 228 (1–3) (2008) 10–29.

[12] T.J. Welgemoed, C.F. Schutte, Capacitive deionization technology™: an alternative desalination solution, Desalination 183 (1–3) (2005) 327–340.
[13] S. Porada, R. Zhao, A. van der Wal, V. Presser, P.M. Biesheuvel, Review on the science and technology of water desalination by capacitive deionization, Prog. Mater. Sci. 58 (8) (2013) 1388–1442.
[14] J.-B. Lee, K.-K. Park, H.-M. Eum, C.-W. Lee, Desalination of a thermal power plant wastewater by membrane capacitive deionization, Desalination 196 (1–3) (2006) 125–134.
[15] P. Xu, J.E. Drewes, D. Heil, G. Wang, Treatment of brackish produced water using carbon aerogel-based capacitive deionization technology, Water Res. 42 (10 − 11) (2008) 2605–2617.
[16] Y.-J. Kim, J.-H. Choi, Enhanced desalination efficiency in capacitive deionization with an ion-selective membrane, Sep. Purif. Technol. 71 (1) (2010) 70–75.
[17] M. Suss, S. Porada, X. Sun, M. Biesheuvel, J. Yoon, V. Presser, Water desalination via capacitive deionization: what is it and what can we expect from it? Energy Environ. Sci. 8 (2015) 2296–2319.
[18] Y. Liu, C. Nie, X. Liu, X. Xu, Z. Sun, L. Pan, Review on carbon-based composite materials for capacitive deionization, RSC Adv. 5 (20) (2015) 15205–15225.
[19] M. Mossad, L. Zou, A study of the capacitive deionisation performance under various operational conditions, J. Hazard. Mater. 213–214 (2012) 491–497.
[20] J.J. Lado, R.E. Pérez-Roa, J.J. Wouters, M.I. Tejedor-Tejedor, C. Federspill, M.A. Anderson, Continuous cycling of an asymmetric capacitive deionization system: an evaluation of the electrode performance and stability, J. Environ. Chem. Eng. 3 (4, Part A) (2015) 2358–2367.
[21] J.J. Lado, R.E. Pérez-Roa, J.J. Wouters, M.I. Tejedor-Tejedor, C. Federspill, J.M. Ortiz, M.A. Anderson, Removal of nitrate by asymmetric capacitive deionization, Sep. Purif. Technol. 183 (2017) 145–152.
[22] L. Wang, P.M. Biesheuvel, S. Lin, Reversible thermodynamic cycle analysis for capacitive deionization with modified Donnan model, J. Colloid Interface Sci. 512 (2018) 522–528.
[23] P.M. Biesheuvel, R. Zhao, S. Porada, A. van der Wal, Theory of membrane capacitive deionization including the effect of the electrode pore space, J. Colloid Interface Sci. 360 (1) (2011) 239–248.
[24] R. Zhao, P.M. Biesheuvel, A. van der Wal, Energy consumption and constant current operation in membrane capacitive deionization, Energy Environ. Sci. 5 (11) (2012) 9520–9527.
[25] T. Kim, J.E. Dykstra, S. Porada, A. van der Wal, J. Yoon, P.M. Biesheuvel, Enhanced charge efficiency and reduced energy use in capacitive deionization by increasing the discharge voltage, J. Colloid Interface Sci. 446 (2015) 317–326.
[26] P. Długołęcki, A. van der Wal, Energy recovery in membrane capacitive deionization, Environ. Sci. Technol. 47 (9) (2013) 4904–4910.
[27] R. Zhao, S. Porada, P.M. Biesheuvel, A. van der Wal, Energy consumption in membrane capacitive deionization for different water recoveries and flow rates, and comparison with reverse osmosis, Desalination 330 (2013) 35–41.
[28] I.C. Karagiannis, P.G. Soldatos, Desalination cost literature: review and assessment, Desalination 223 (1) (2008) 448–456.
[29] A.M. Johnson, J. Newman, Desalting by means of porous carbon electrodes, J. Electrochem. Soc. 118 (3) (1971) 510–517.
[30] J.S. Newman, C.W. Tobias, Theoretical analysis of current distribution in porous electrodes, J. Electrochem. Soc. 109 (12) (1962) 1183–1191.
[31] R. Zhao, P.M. Biesheuvel, H. Miedema, H. Bruning, A. van der Wal, Charge efficiency: a functional tool to probe the double-layer structure inside of porous electrodes and application in the modeling of capacitive deionization, J. Phys. Chem. Lett. 1 (1) (2009) 205–210.
[32] P.M. Biesheuvel, Thermodynamic cycle analysis for capacitive deionization, J. Colloid Interface Sci. 332 (1) (2009) 258–264.
[33] P.M. Biesheuvel, Limpt Bv, Wal Avd, Dynamic adsorption/desorption process model for capacitive deionization, J. Phys. Chem. C 113 (2009) 5636–5640.
[34] P.M. Biesheuvel, A. van der Wal, Membrane capacitive deionization, J. Membr. Sci. 346 (2) (2010) 256–262.
[35] P.M. Biesheuvel, M.Z. Bazant, Nonlinear dynamics of capacitive charging and desalination by porous electrodes, Phys. Rev. E 81 (3) (2010) 031502.
[36] B.B. Sales, M. Saakes, J.W. Post, C.J.N. Buisman, P.M. Biesheuvel, H.V.M. Hamelers, Direct power production from a water salinity difference in a membrane-modified supercapacitor flow cell, Environ. Sci. Technol. 44 (14) (2010) 5661–5665.
[37] P.M. Biesheuvel, Y. Fu, M.Z. Bazant, Diffuse charge and Faradaic reactions in porous electrodes, Phys. Rev. E 83 (6) (2011) 061507.
[38] P.M. Biesheuvel, Y. Fu, M.Z. Bazant, Electrochemistry and capacitive charging of porous electrodes in asymmetric multicomponent electrolytes, Russ. J. Electrochem. 48 (6) (2012) 580–592.
[39] P. Biesheuvel, S. Porada, M. Levi, M.Z. Bazant, Attractive forces in microporous carbon electrodes for capacitive deionization, J. Solid State Electrochem. 18 (5) (2014) 1365–1376.
[40] E.N. Guyes, A.N. Shocron, A. Simanovski, P.M. Biesheuvel, M.E. Suss, A one-dimensional model for water desalination by flow-through electrode capacitive deionization, Desalination 415 (2017) 8–13.
[41] C.A.R. Perez, O.N. Demirer, R.L. Clifton, R.M. Naylor, C.H. Hidrovo, Macro analysis of the electro-adsorption process in low concentration NaCl solutions for water desalination applications, J. Electrochem. Soc. 160 (3) (2013) E13–E21.
[42] P. Biesheuvel, Activated Carbon is an Electron-conducting Amphoteric Ion Adsorbent, arXiv preprint arXiv:150906354 (2015).
[43] P.M. Biesheuvel, H.V.M. Hamelers, M.E. Suss, Theory of water desalination by porous electrodes with immobile chemical charge, Colloids Interface Sci. Commun. 9 (2015) 1–5.
[44] J.E. Dykstra, R. Zhao, P.M. Biesheuvel, A. van der Wal, Resistance identification and rational process design in capacitive deionization, Water Res. 88 (2016) 358–370.
[45] J.E. Dykstra, K.J. Keesman, P.M. Biesheuvel, A. van der Wal, Theory of pH changes in water desalination by capacitive deionization, Water Res. 119 (2017) 178–186.
[46] A. Hemmatifar, M. Stadermann, J.G. Santiago, Two-dimensional porous electrode model for capacitive deionization, J. Phys. Chem. C 119 (44) (2015) 24681–24694.
[47] R. Zhao, O. Satpradit, H.H.M. Rijnaarts, P.M. Biesheuvel, A. van der Wal, Optimization of salt adsorption rate in membrane capacitive deionization, Water Res. 47 (5) (2013) 1941–1952.
[48] A. Soffer, M. Folman, The electrical double layer of high surface porous carbon electrode, J. Electroanal. Chem. Interfacial Electrochem. 38 (1) (1972) 25–43.
[49] E. Avraham, Y. Bouhadana, A. Soffer, D. Aurbach, Limitation of charge efficiency in capacitive deionization: I. On the behavior of single activated carbon, J. Electrochem. Soc. 156 (6) (2009) P95–P99.
[50] J.C. Farmer, D.V. Fix, G.V. Mack, R.W. Pekala, J.F. Poco, Capacitive deionization of NaCl and $NaNO_3$ solutions with carbon aerogel electrodes, J. Electrochem. Soc. 143 (1) (1996) 159–169.
[51] J.C. Farmer, S.M. Bahowick, J.E. Harrar, D.V. Fix, R.E. Martinelli, A.K. Vu, K.L. Carroll, Electrosorption of chromium ions on carbon aerogel electrodes as a means of remediating ground water, Energy Fuel 11 (2) (1997) 337–347.
[52] S. Porada, L. Borchardt, M. Oschatz, M. Bryjak, J.S. Atchison, K.J. Keesman, S. Kaskel, P.M. Biesheuvel, V. Presser, Direct prediction of the desalination performance of porous carbon electrodes for capacitive deionization, Energy Environ. Sci. 6 (12) (2013) 3700–3712.
[53] S. Porada, L. Weinstein, R. Dash, A. van der Wal, M. Bryjak, Y. Gogotsi, P.M. Biesheuvel, Water desalination using capacitive deionization with microporous carbon electrodes, ACS Appl. Mater. Interfaces 4 (3) (2012) 1194–1199.
[54] S. Porada, F. Schipper, M. Aslan, M. Antonietti, V. Presser, T.-P. Fellinger, Capacitive deionization using biomass-based microporous salt-templated heteroatom-doped carbons, ChemSusChem 8 (11) (2015) 1867–1874.
[55] K. Laxman, M.T.Z. Myint, R. Khan, T. Pervez, J. Dutta, Improved desalination by zinc oxide nanorod induced electric field enhancement in capacitive deionization of brackish water, Desalination 359 (Supplement C) (2015) 64–70.
[56] J. Lee, S. Kim, C. Kim, J. Yoon, Hybrid capacitive deionization to enhance the desalination performance of capacitive techniques, Energy Environ. Sci. 7 (11) (2014) 3683–3689.
[57] M.E. Suss, T.F. Baumann, W.L. Bourcier, C.M. Spadaccini, K.A. Rose, J.G. Santiago, M. Stadermann, Capacitive desalination with flow-through electrodes, Energy Environ. Sci. 5 (11) (2012) 9511–9519.
[58] Y.-J. Kim, J.-H. Choi, Improvement of desalination efficiency in capacitive deionization using a carbon electrode coated with an ion-exchange polymer, Water Res. 44 (3) (2010) 990–996.
[59] S. Porada, D. Weingarth, H.V.M. Hamelers, M. Bryjak, V. Presser, P.M. Biesheuvel, Carbon flow electrodes for continuous operation of capacitive deionization and capacitive mixing energy generation, J. Mater. Chem. A 2 (24) (2014) 9313–9321.
[60] L. Han, K.G. Karthikeyan, M.A. Anderson, J.J. Wouters, K.B. Gregory, Mechanistic insights into the use of oxide nanoparticles coated asymmetric electrodes for capacitive deionization, Electrochim. Acta 90 (2013) 573–581.
[61] H. Li, L. Zou, Ion-exchange membrane capacitive deionization: a new strategy for brackish water desalination, Desalination 275 (1–3) (2011) 62–66.
[62] I. Cohen, E. Avraham, M. Noked, A. Soffer, D. Aurbach, Enhanced charge efficiency in capacitive deionization achieved by surface-treated electrodes and by means of a third electrode, J. Phys. Chem. C 115 (40) (2011) 19856–19863.
[63] E. García-Quismondo, C. Santos, J. Soria, J. Palma, M.A. Anderson, New operational modes to increase energy efficiency in capacitive deionization systems, Environ. Sci. Technol. 50 (11) (2016) 6053–6060.
[64] J. Zhang, K.B. Hatzell, M.C. Hatzell, A combined heat- and power-driven membrane capacitive deionization system, Environ. Sci. Technol. Lett. 4 (11) (2017) 470–474.
[65] R.F. Probstein, Physicochemical Hydrodynamics: An Introduction, John Wiley & Sons, 2005.
[66] K. Dermentzis, A. Davidis, C. Chatzichristou, A. Dermentzi, Ammonia removal from fertilizer plant effluents by a coupled electrostatic shielding based electrodialysis/electrodeionization process, J 14 (2012) 468–476.
[67] A. Bejan, Advanced Engineering Thermodynamics, John Wiley & Sons, 2016.
[68] Y. Qu, T.F. Baumann, J.G. Santiago, M. Stadermann, Characterization of resistances of a capacitive deionization system, Environ. Sci. Technol. 49 (16) (2015) 9699–9706.
[69] S.A. Hawks, J.M. Knipe, P.G. Campbell, C.K. Loeb, M.A. Hubert, J.G. Santiago, M. Stadermann, Quantifying the flow efficiency in constant-current capacitive deionization, Water Res. 129 (2018) 327–336.
[70] E. García-Quismondo, C. Santos, J. Lado, J. Palma, M.A. Anderson, Optimizing the energy efficiency of capacitive deionization reactors working under real-world conditions, Environ. Sci. Technol. 47 (20) (2013) 11866–11872.
[71] T. Alencherry, A.R. Naveen, S. Ghosh, J. Daniel, R. Venkataraghavan, Effect of increasing electrical conductivity and hydrophilicity on the electrosorption capacity of activated carbon electrodes for capacitive deionization, Desalination 415 (2017) 14–19.
[72] A.G. El-Deen, J.-H. Choi, C.S. Kim, K.A. Khalil, A.A. Almajid, N.A.M. Barakat, TiO_2 nanorod-intercalated reduced graphene oxide as high performance electrode material for membrane capacitive deionization, Desalination 361 (2015) 53–64.
[73] Jeon S-i, Park H-r, Yeo J-g, S. Yang, C.H. Cho, M.H. Han, D.K. Kim, Desalination via a new membrane capacitive deionization process utilizing flow-electrodes, Energy Environ. Sci. 6 (5) (2013) 1471–1475.
[74] L. Wang, S. Lin, Intrinsic tradeoff between kinetic and energetic efficiencies in membrane capacitive deionization, Water Res. 129 (2018) 394–401.